

Transition Zone in the Context

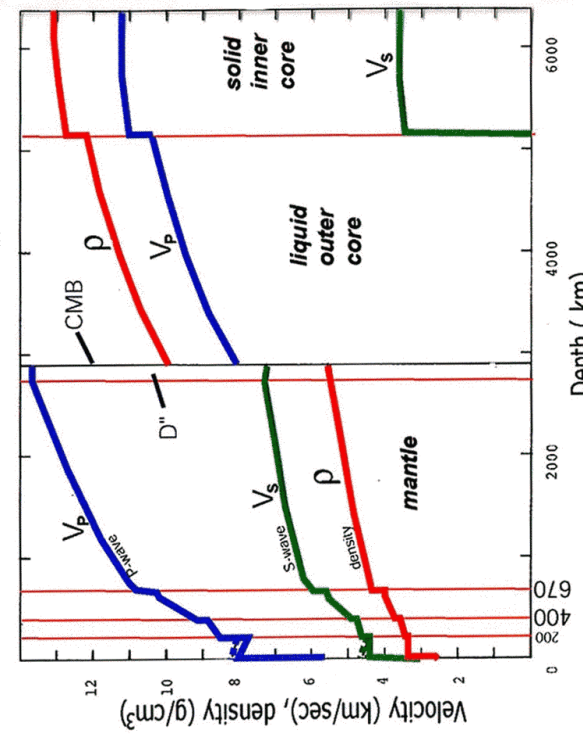
.....

Adam M. Dziewonski

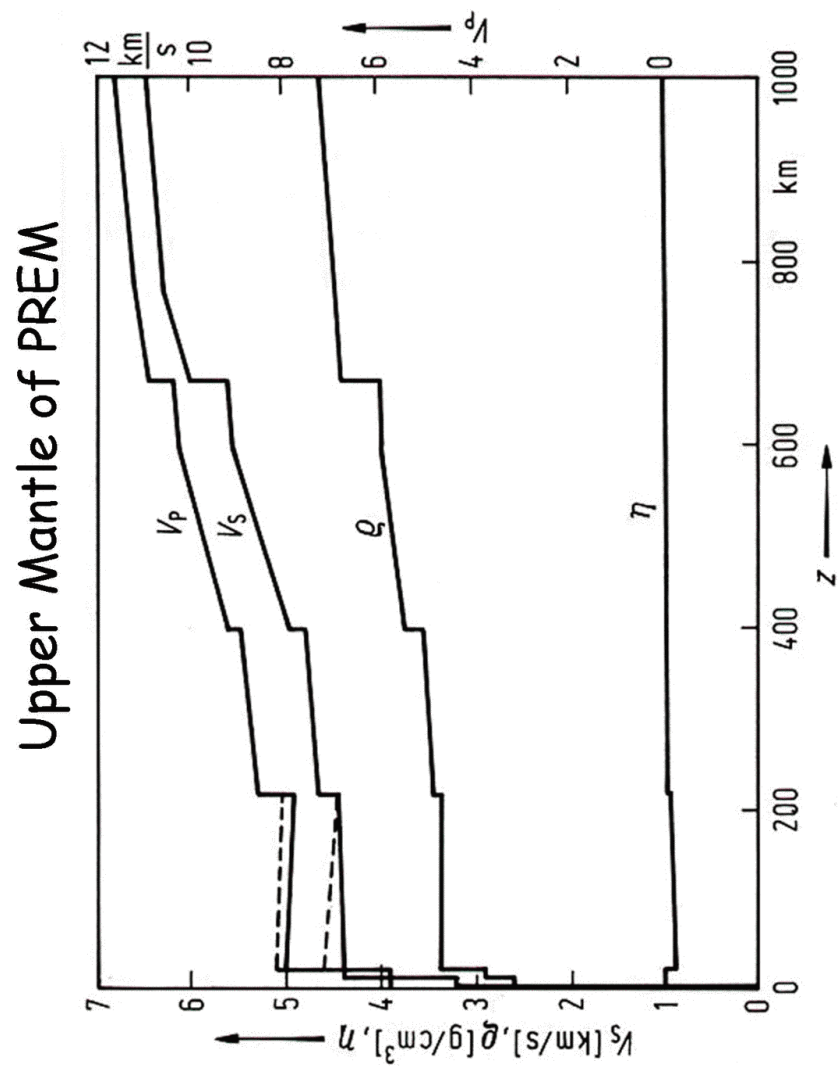
July 29, 2006

CIDER at KITP

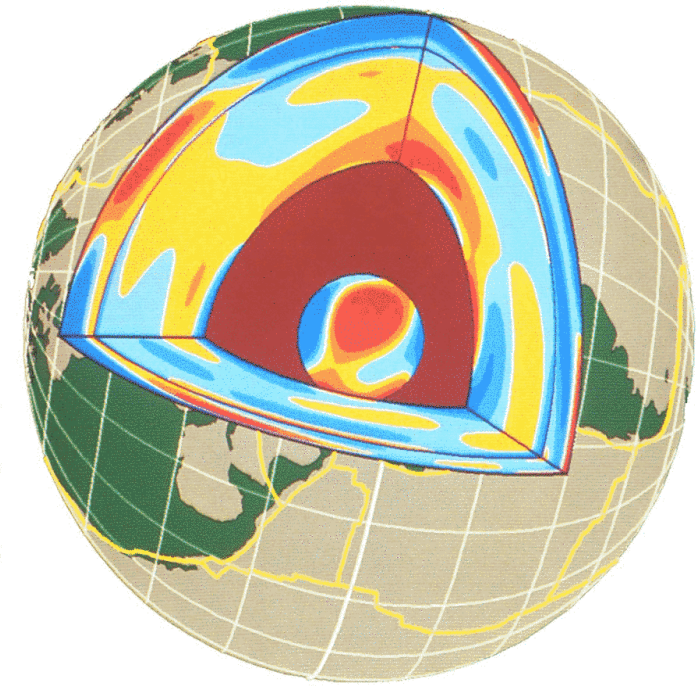
The PREM Model

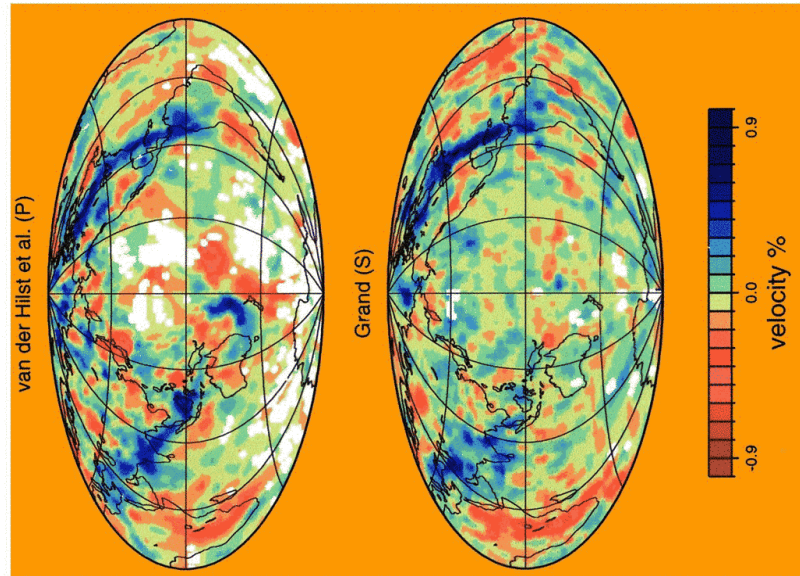


PREM was obtained using nearly 1000 normal mode and a wide range of travel time phases. After 22 years, it is still widely used as a reference model.



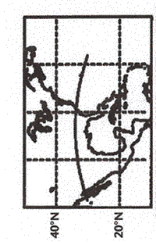
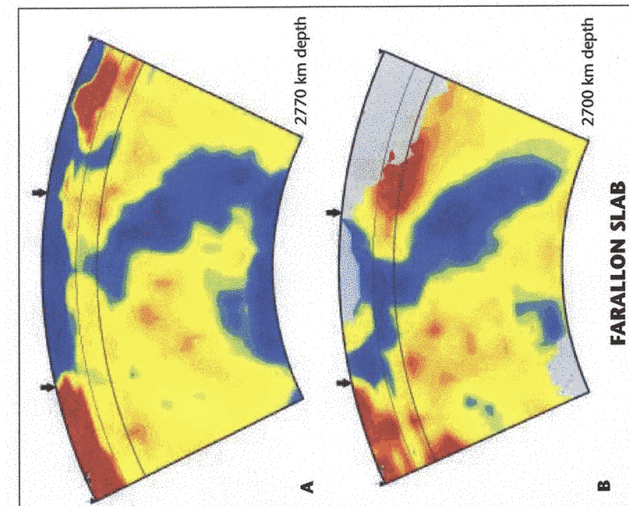
3-D Tomography Allows a New Look





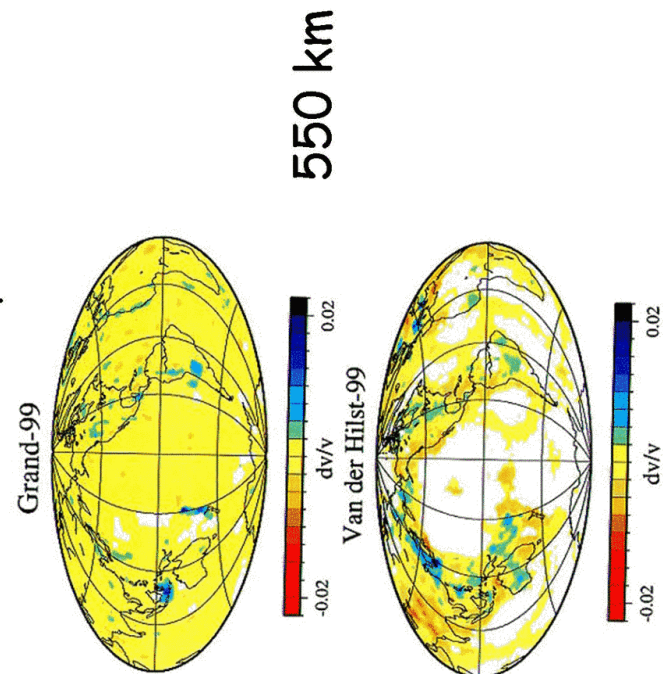
P- and S-velocity
anomalies at 1300
km depth

Slab Penetration into the Lower Mantle

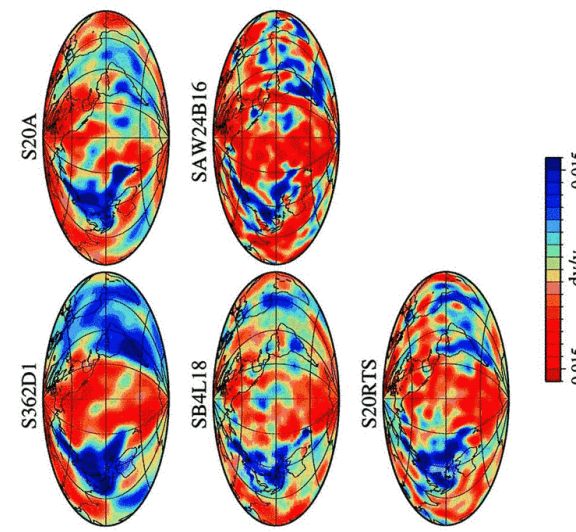


Grand and v. d. Hilst, 1997

Transition Zone Velocity Anomalies



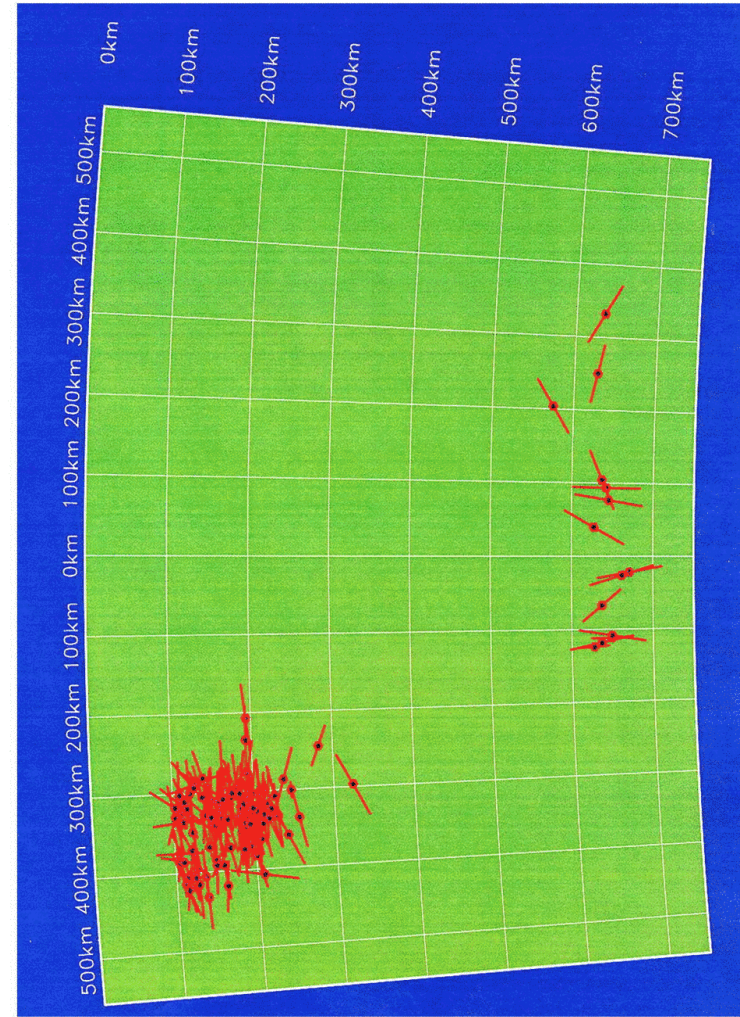
550 km depth



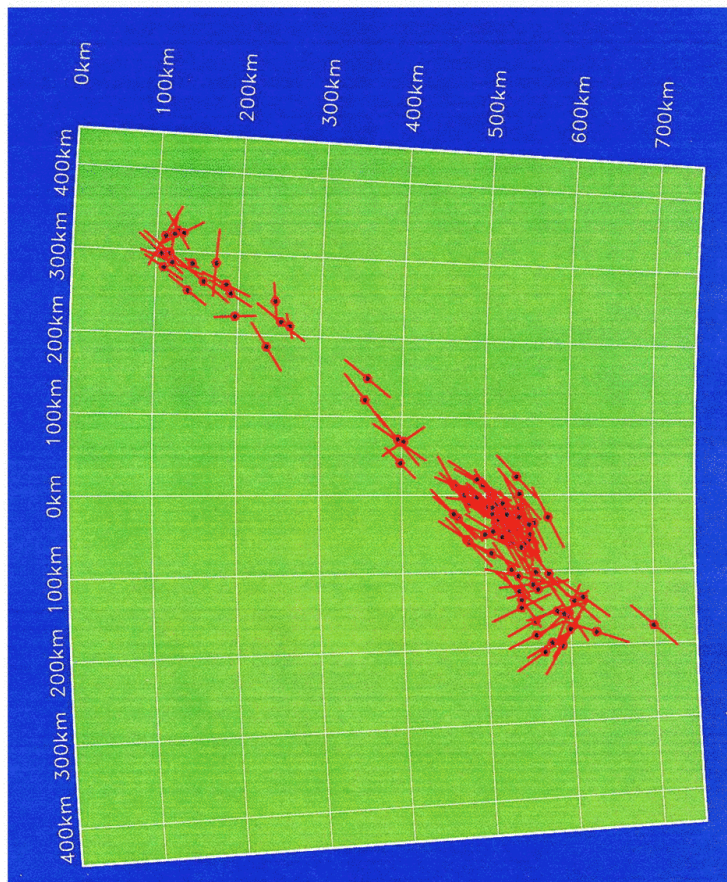
Shear Velocity Anomalies
in the Transition
Zone Obtained Using
Surface Wave and/or
Waveform Data

Earthquakes Outside Slabs

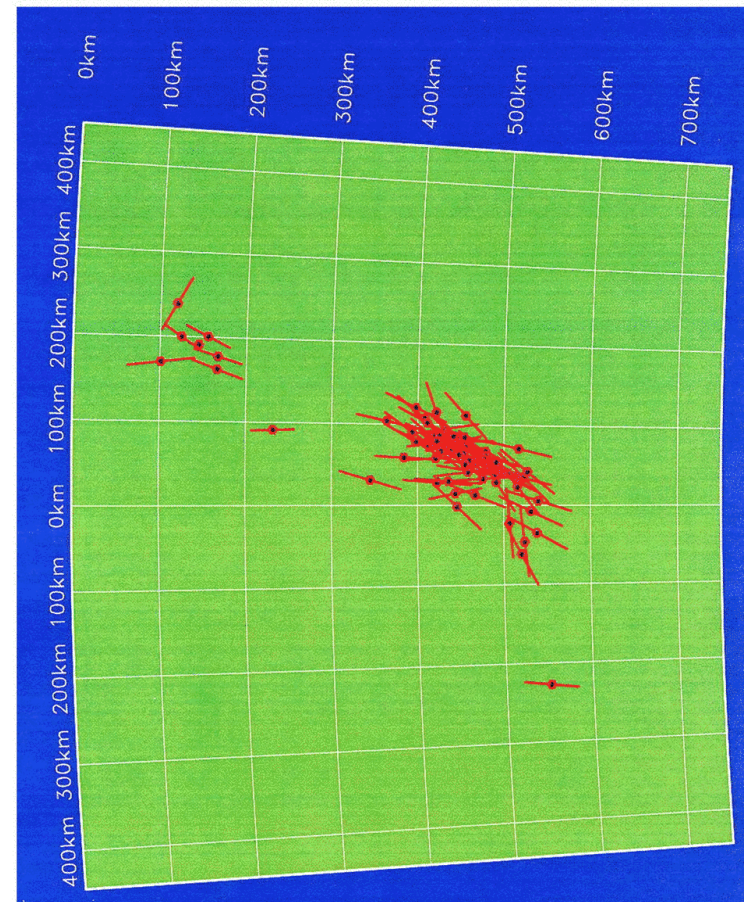
Fiji Plateau



Central Tonga-Kermadec



Izu-Bonin



Early Plate Tectonics; Flow Limited to Upper mantle

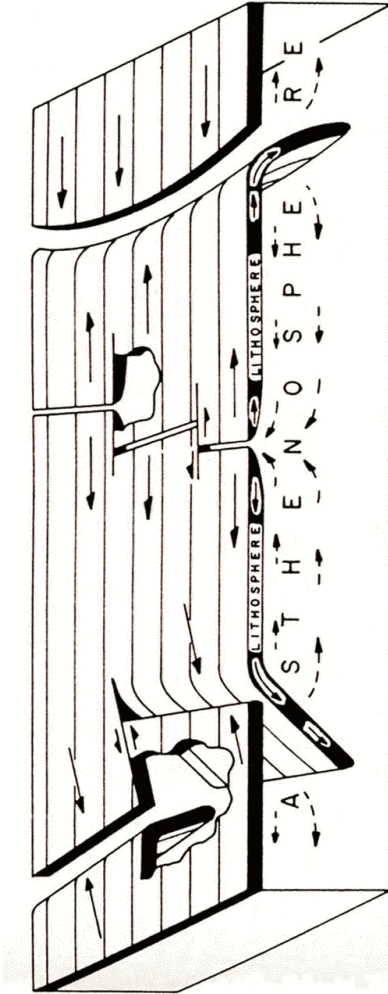
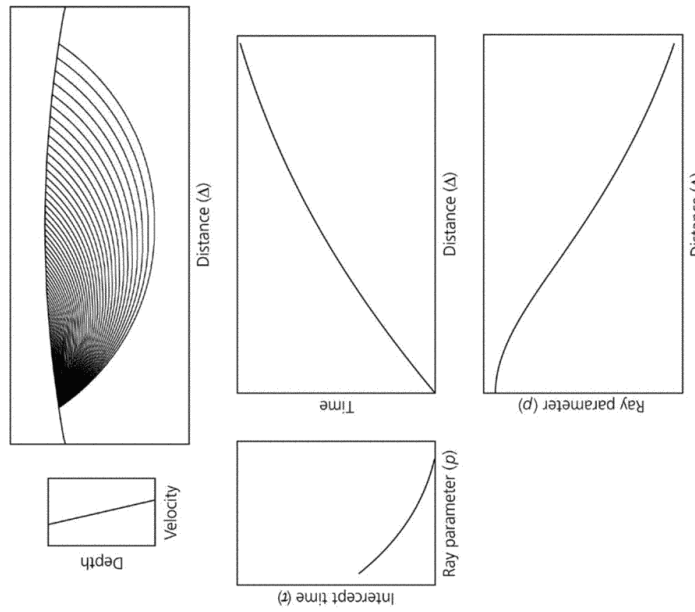


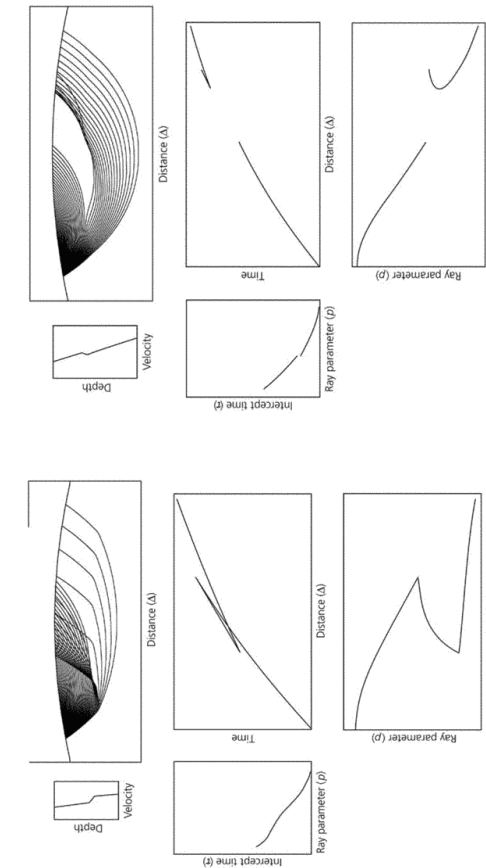
FIGURE 42 The Isacks-Oliver-Sykes model of plate configurations. Plates are created from the asthenosphere at mid-oceanic ridges, cool, and thicken to 70–150 kilometers to form the lithosphere as they slide over the asthenosphere and move away from the ridges; they reenter the asthenosphere at subduction zones.

Velocity Anomalies in the Transition Zone

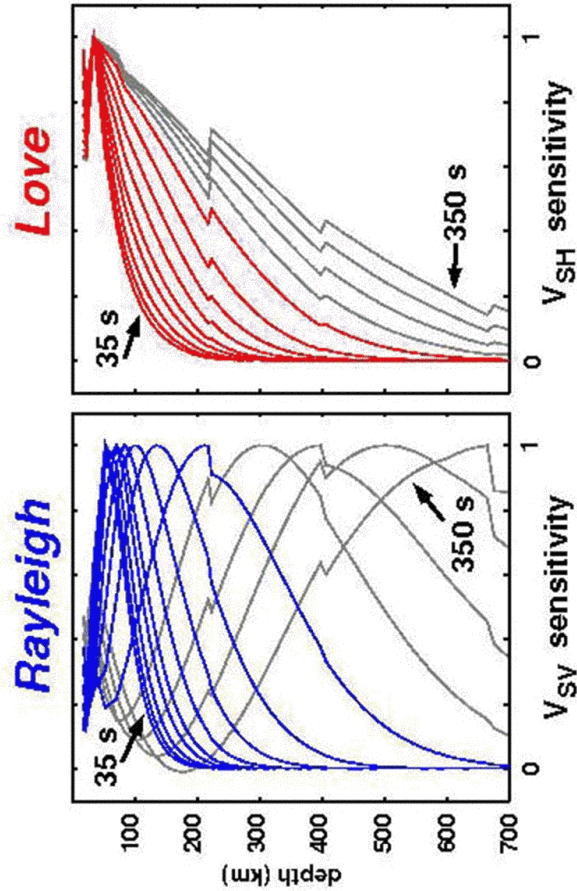
Seismic Rays in a Smooth Medium



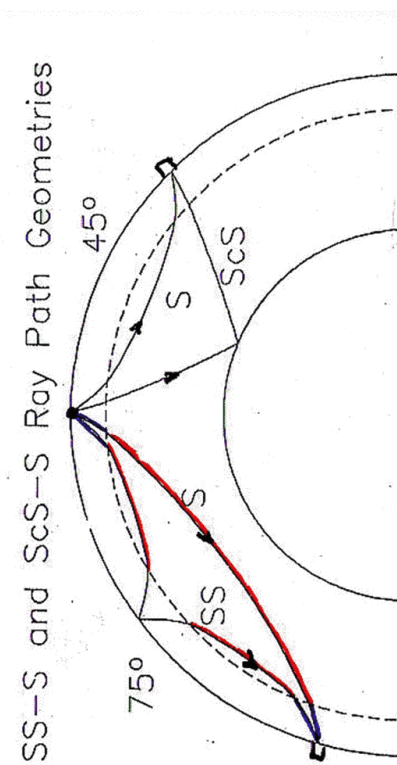
Rays in a Medium with Steep Gradients and a Low Velocity Zone

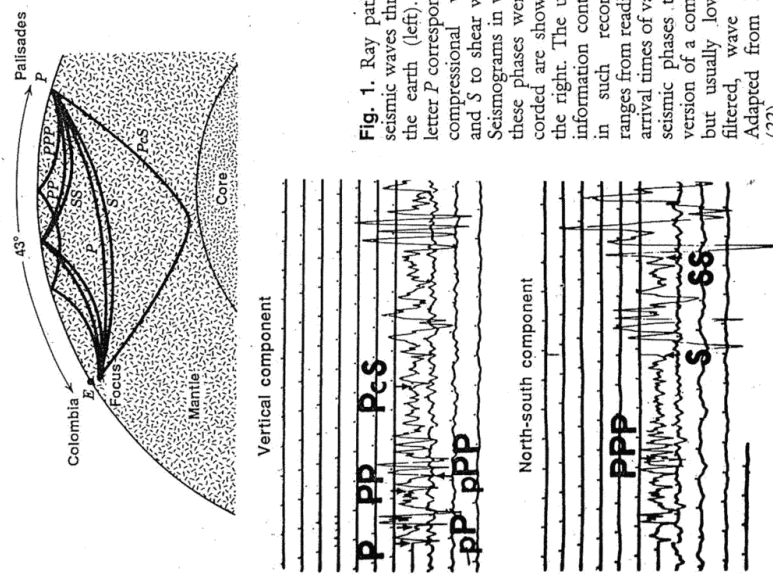


Surface Wave Sensitivity Kernels



Differential Travel Times



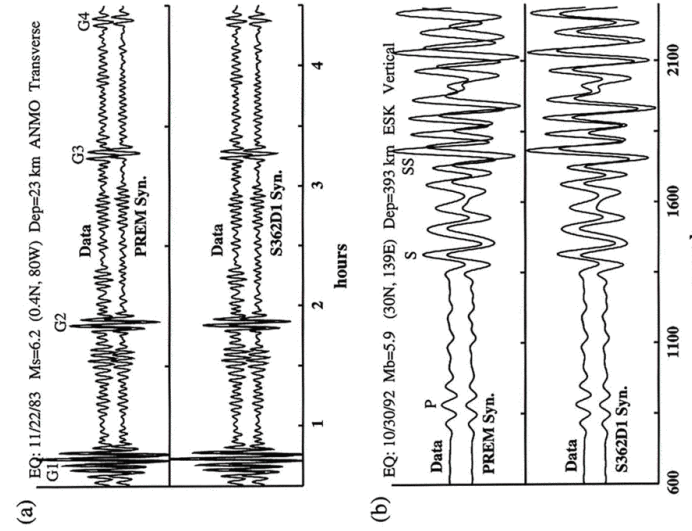


A single seismogram contains information on the Earth's structure along many paths

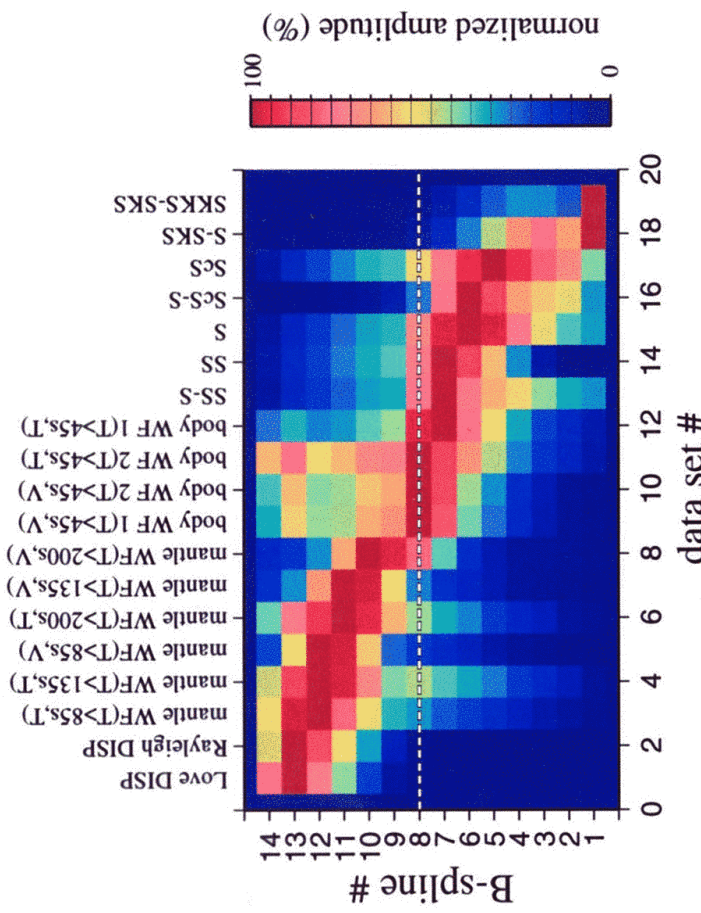
Fig. 1. Ray paths of seismic waves through the earth (left). The letter *P* corresponds to compressional waves and *S* to shear waves. Seismograms in which these phases were recorded are shown on the right. The use of information contained in such recordings ranges from reading of arrival times of various seismic phases to inversion of a complete, but usually low-pass filtered, wave train. Adapted from Dorn (22).

Waveform Inversion

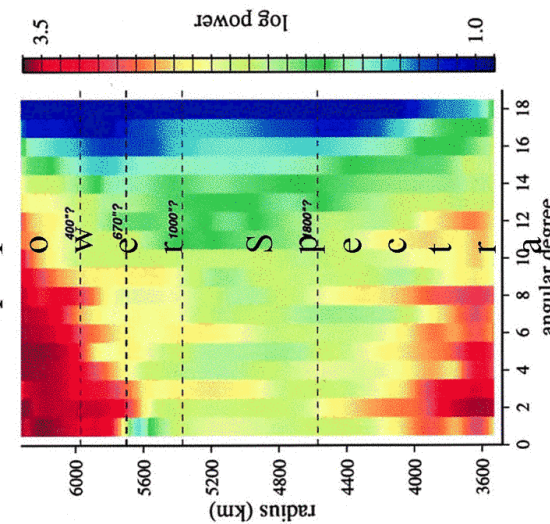
Entire seismograms can be inverted directly into structural perturbations. Mantle wave (top) and body wave (bottom) are significantly better fit by a 3-D model S362D1 (Gu et al., 2001)



Maximum Resolution of Different Data Types



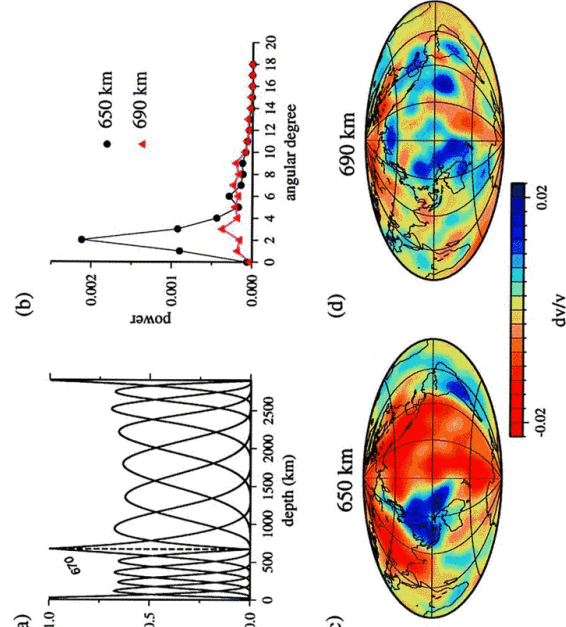
Power Spectra of Model S362CO



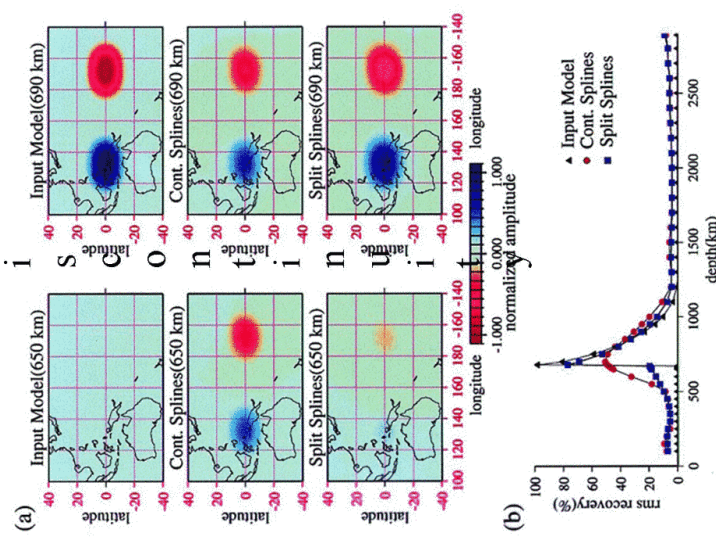
1. Upper mantle: strong and red -- thermal boundary (deg. 5) and transition zone (deg. 2).
2. Middle mantle: weak and white.
3. Lowermost mantle: strong and red (degree 2)

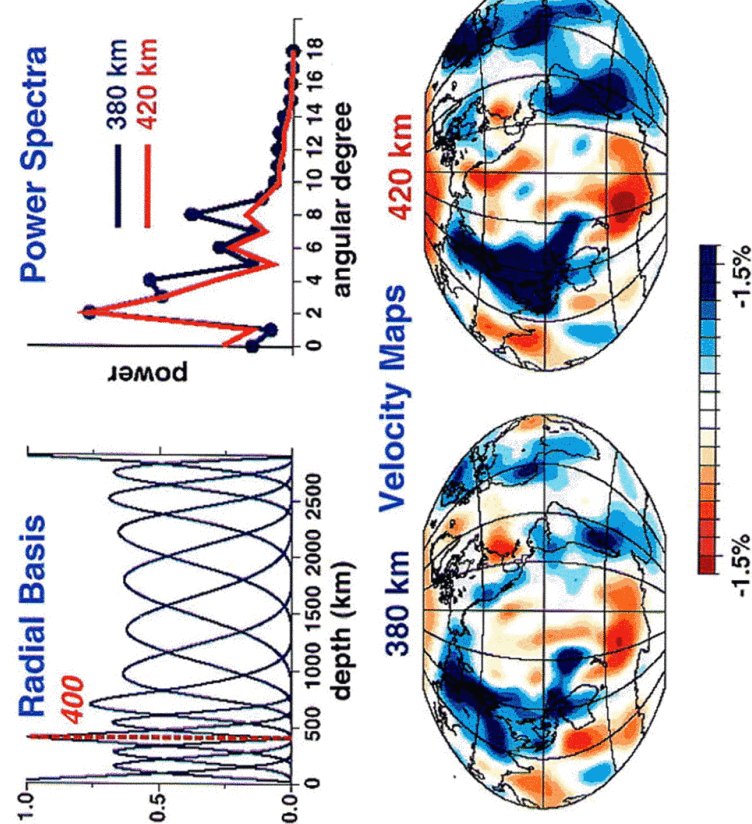
Abrupt spectrum change at 660 km

When a discontinuity at 660 km is allowed, we obtain very different images above and below it. From Gu *et al.*, 2001.

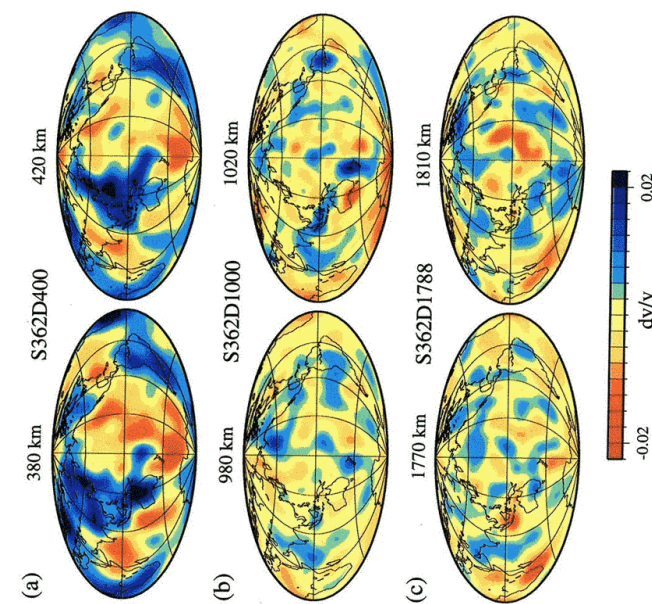


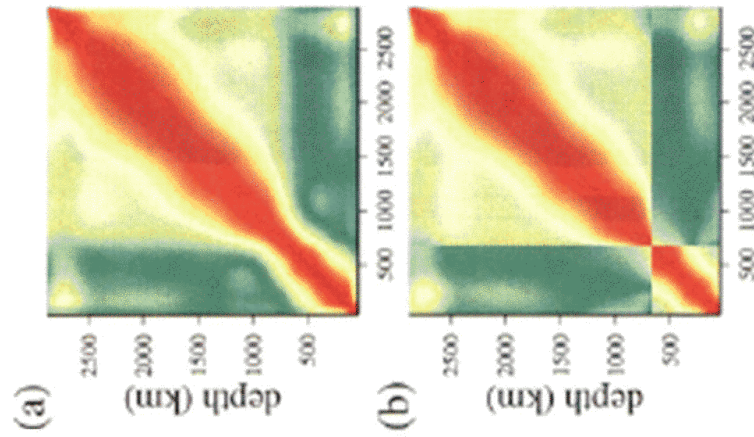
Discontinuity Resolution Test





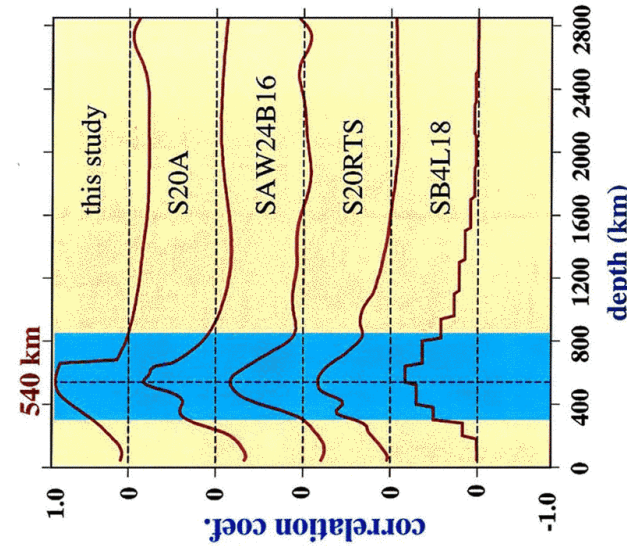
Experiments with introducing the discontinuity at other depths did not produce similar results





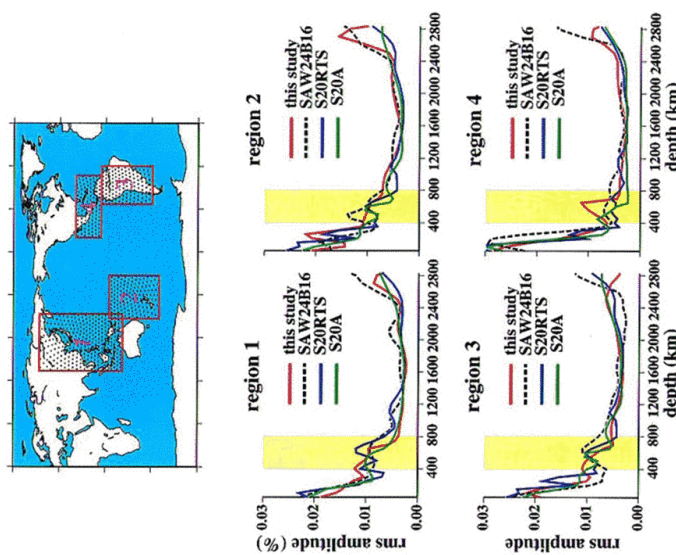
Radial correlation functions
of models S361C and S361D

Radial correlation function



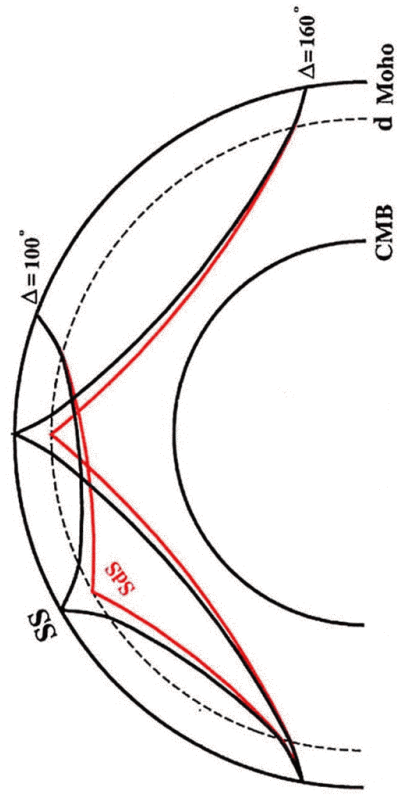
Radial correlation function (Jordan *et al.*, 1994) is used to measure average depth interval over which the structure changes. The transition zone structure changes rapidly in all models on the right except for SB4L18.

Regional Velocity RMS



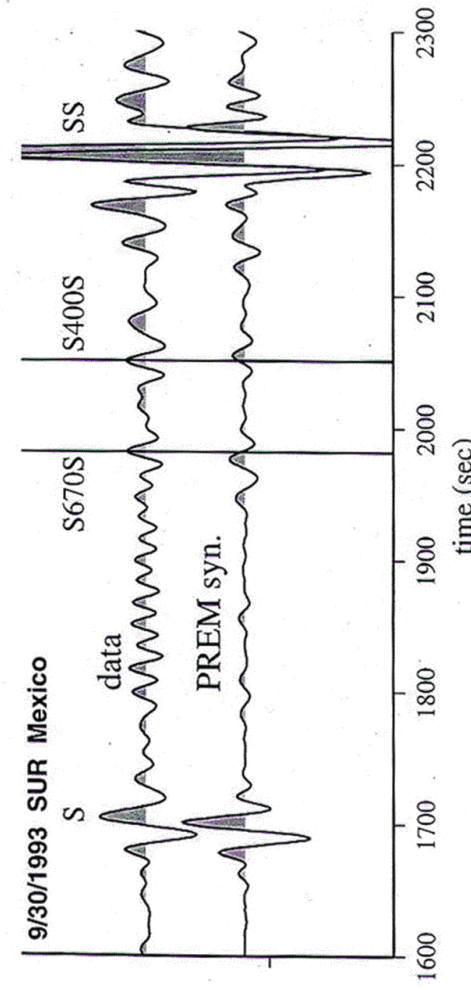
Topography of UM Discontinuities

Differential TT: SS - SdS

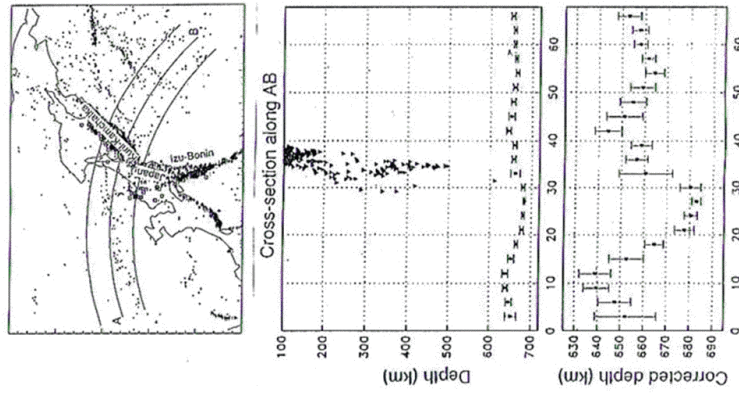


Ray paths of SS and precursors of SdS for distances of 100° and 160°, calculated using PREM [Dziewonski and Anderson, 1981]. The trajectories are very similar away from the reflection point. The discontinuity labeled by “d” in this demonstration is the 660-km discontinuity.

Observed and Predicted Arrival Times of the Precursors

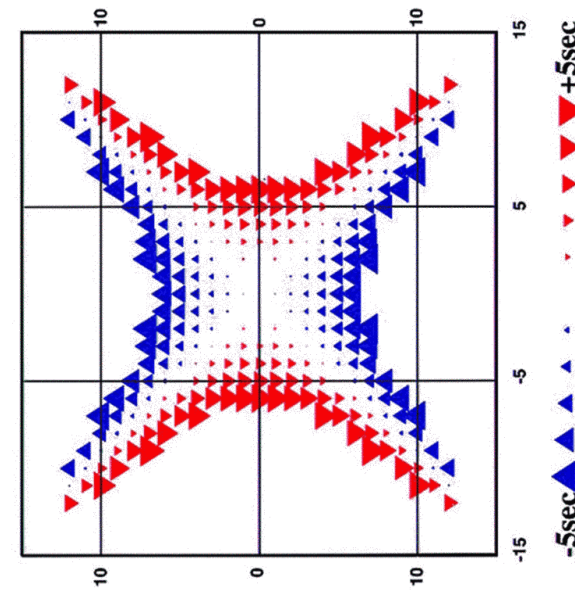


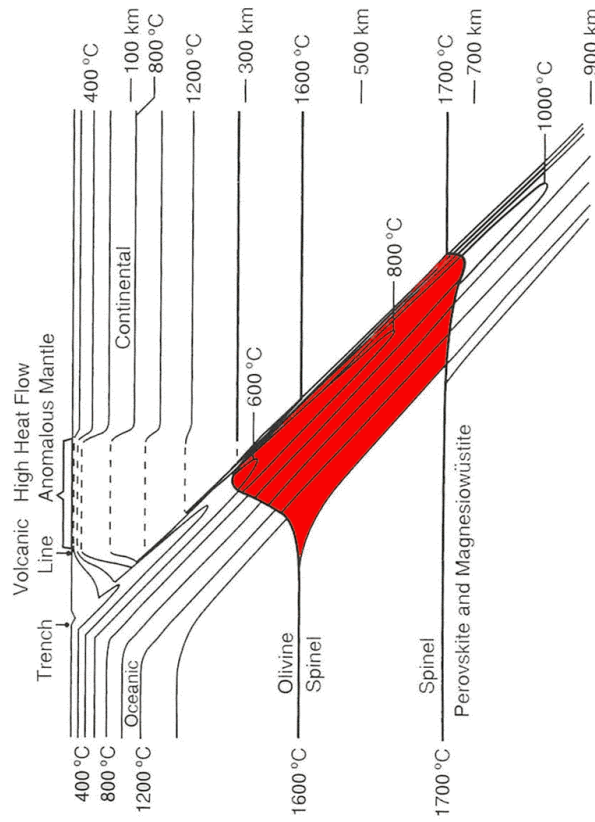
First global study of
the 660 km
Discontinuity:
Shearer and
Masters (1992)



Travel Time Fresnel Zone

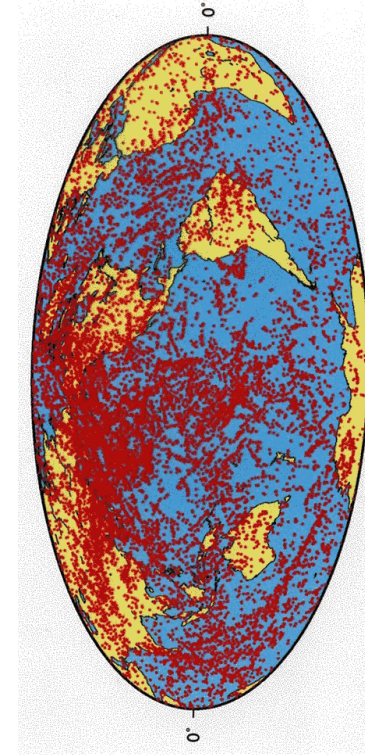
Period = 20 sec, $\Delta = 120^\circ$





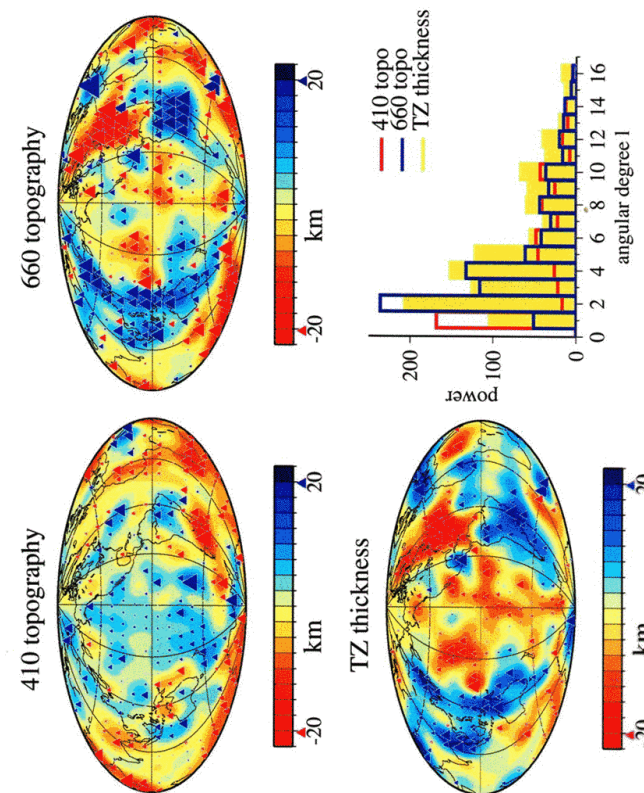
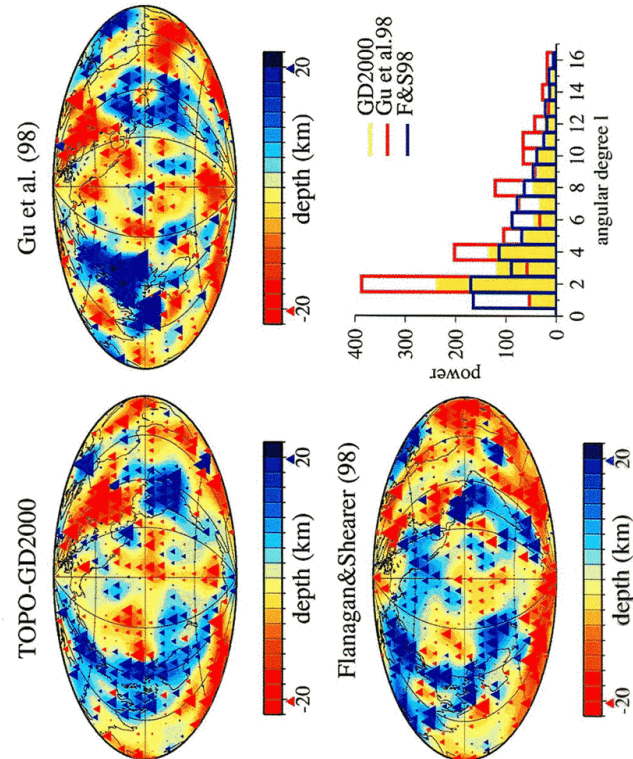
Local variations, such as within the slab, could not be resolved with this technique because of the averaging (smoothing) scheme and the size of the Fresnel zone.

SS - SdS precursors: a tool to study upper mantle discontinuities



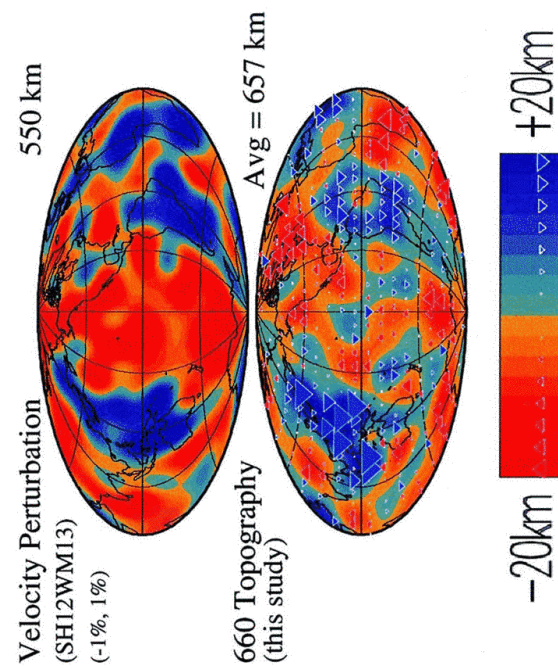
SS-SdS precursors are used to study the presence and topography of upper mantle discontinuities such as 220 km (Lehmann), 410, 520 (?) and 650 km. In contrast with the "receiver functions", they can be used in places where there are no receivers. The dots show mid-point reflections of 21,000 seismograms used in analysis.

Three different studies of the 660 km topography

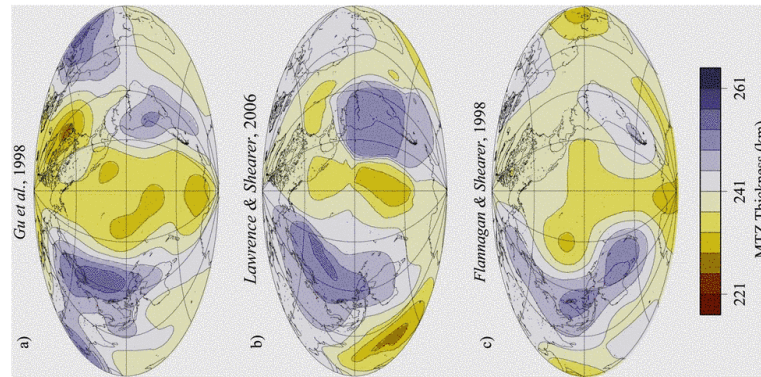


Inversion of SS - SdS data for the topography of 410 and 660 km discontinuities and an independent estimate of TZ thickness from direct cross-correlation of S400S with S670S waveforms.

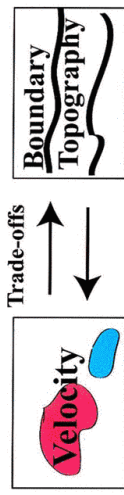
Correlation of TZ velocity anomalies and 660 topography



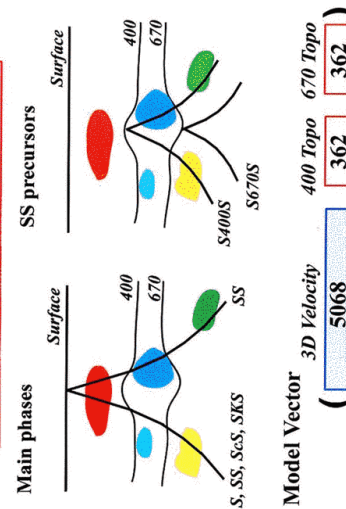
High correlation of the 660km discontinuity topography with velocity perturbations in the transition zone indicates ponding of heavier (cooler) material. There is no correlation with the anomalies below 660km.



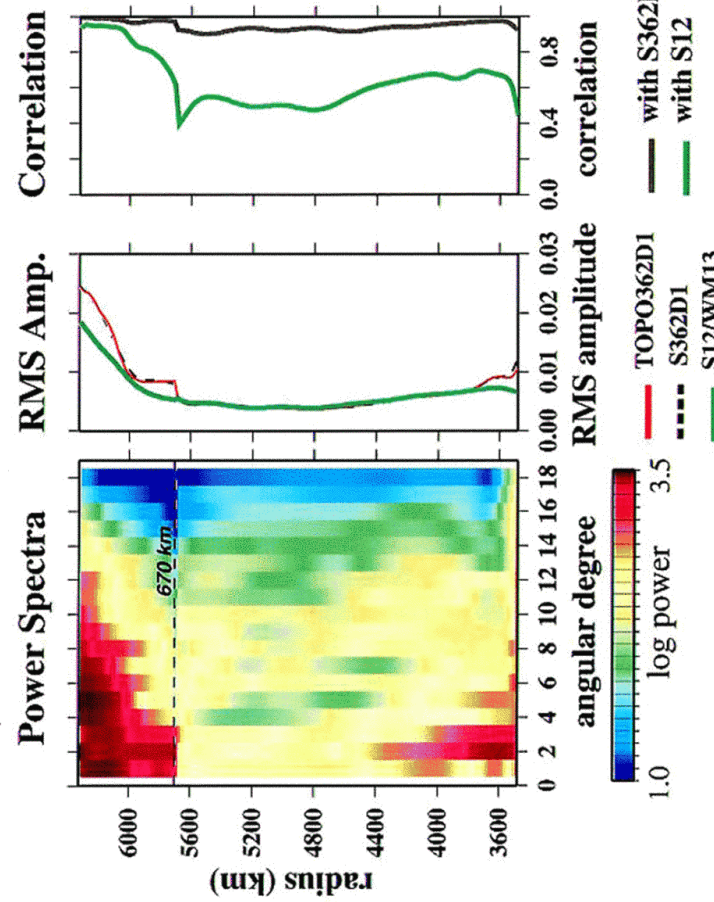
Additional comparisons of TZ thickness; the middle figure is obtained using converted waves

Problem:**Solution:**

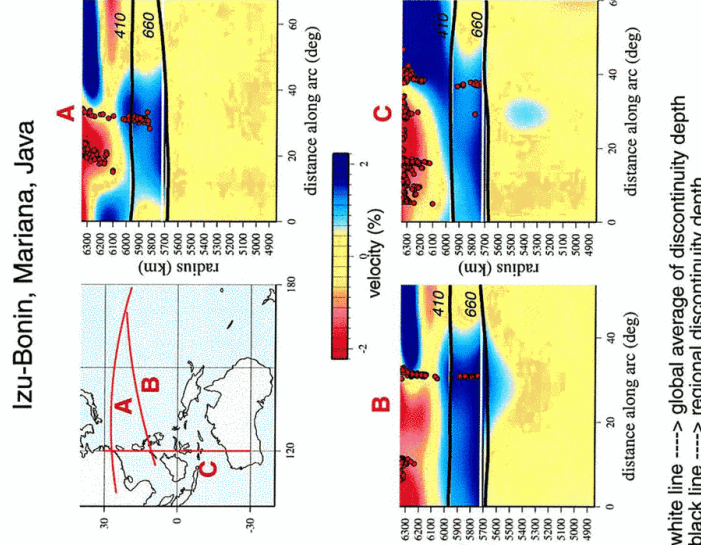
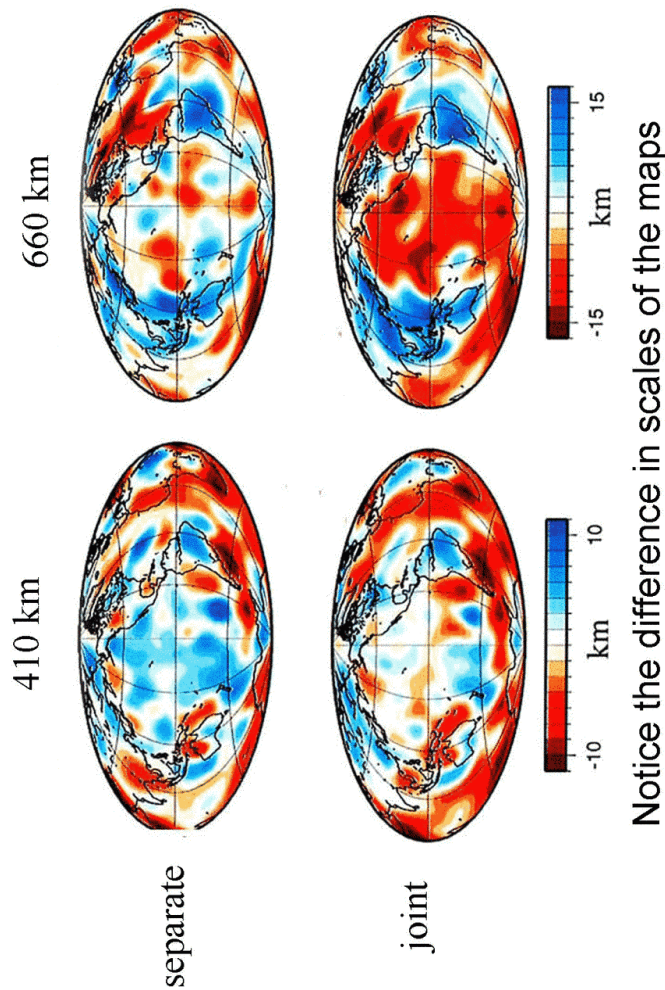
$$\text{Residual} = 3D + 400 \text{ Topo} + 670 \text{ Topo}$$



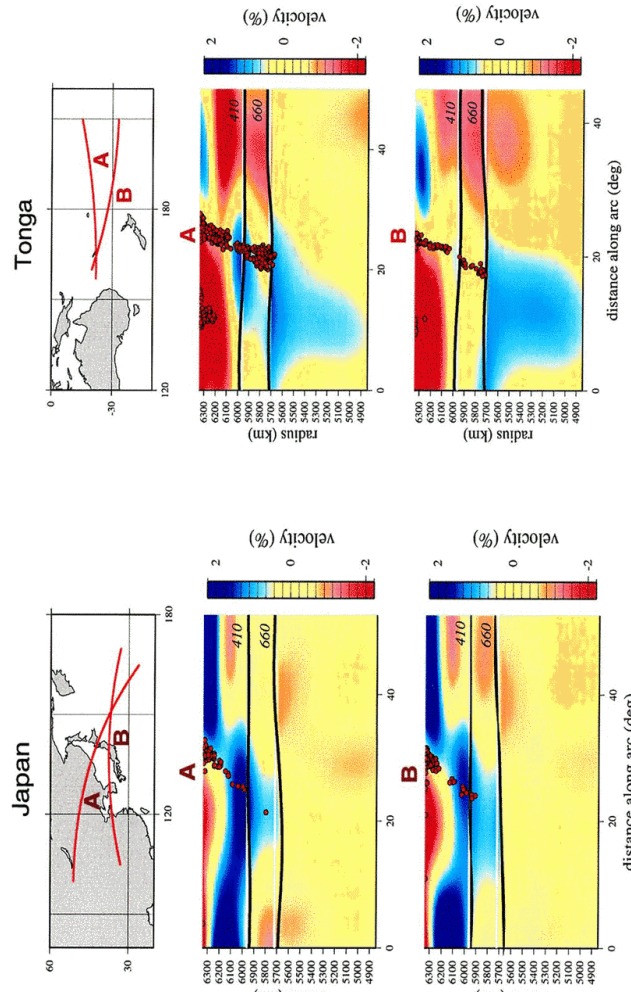
To avoid possible tradeoffs between the velocity anomalies and topography of the discontinuities we perform a joint inversion for a 3D velocity model and the boundary topographies



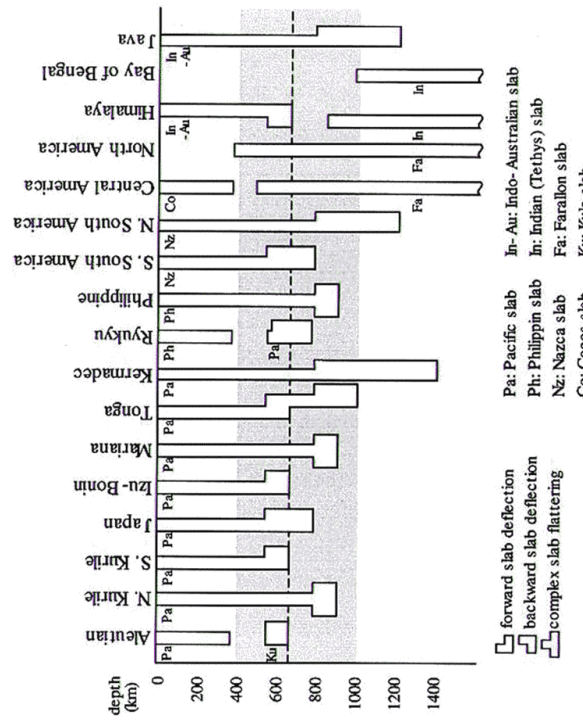
Joint inversion diminishes the topography of the 410 km discontinuity and enhances that of 660 km discontinuity



Cross-sections in the Western Pacific show extended high velocity anomalies in the transition zone, with little or no continuation into the lower mantle



Cross-sections through other subduction zones show different signatures. Notice the depth of anomalies under the Tonga.



Depth of penetration of subducted slabs. From Fukao et al., 2001

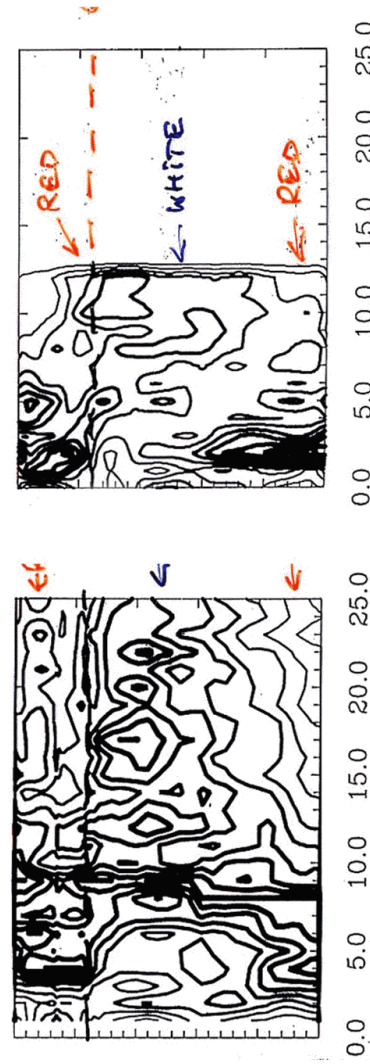
Mantle convection



Tackley et al., 1993

Behavior of the power spectra as a function of depth for a simulated mantle convection with a phase change boundary and a tomographic model (Su et al., 1994) is very similar.

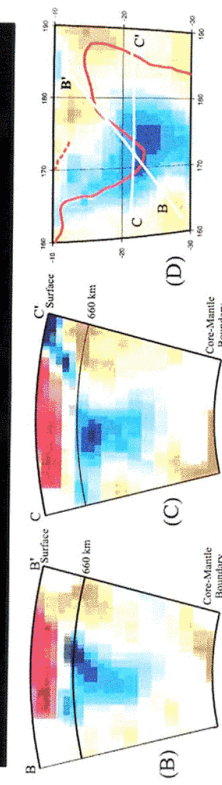
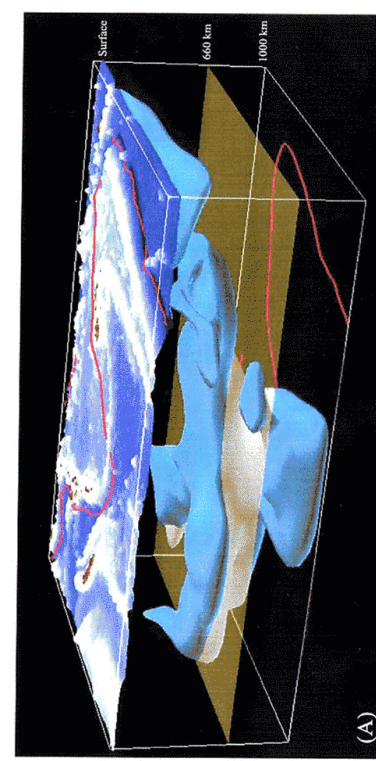
Mantle convection



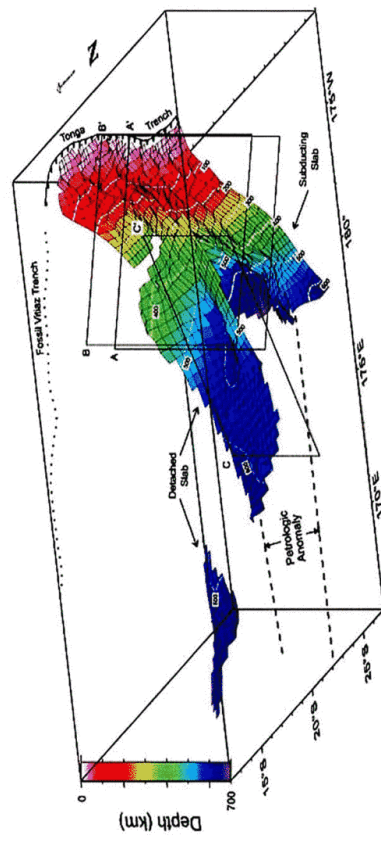
From Tackley et al., 1994

Lower Mantle

Vanuatu-Fiji-Tonga anomaly

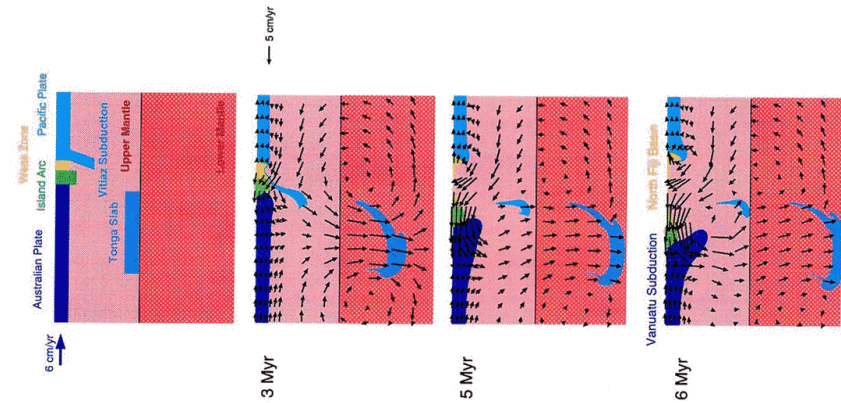


Tonga, 3-D seismicity



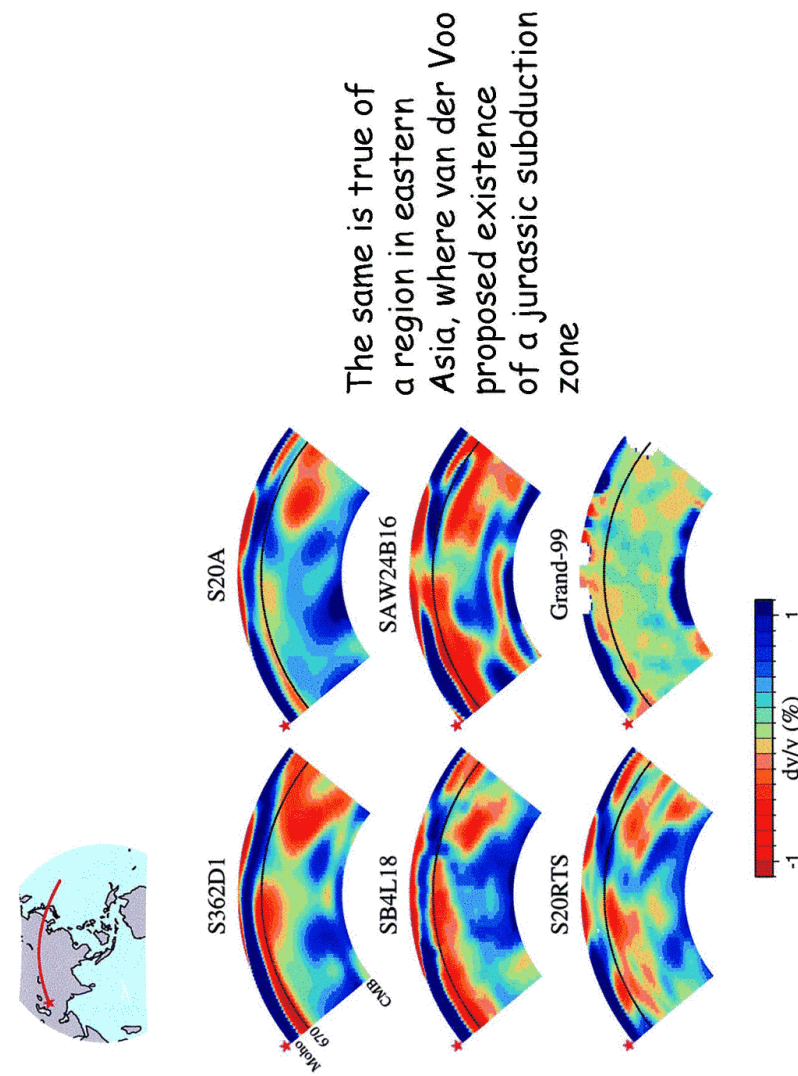
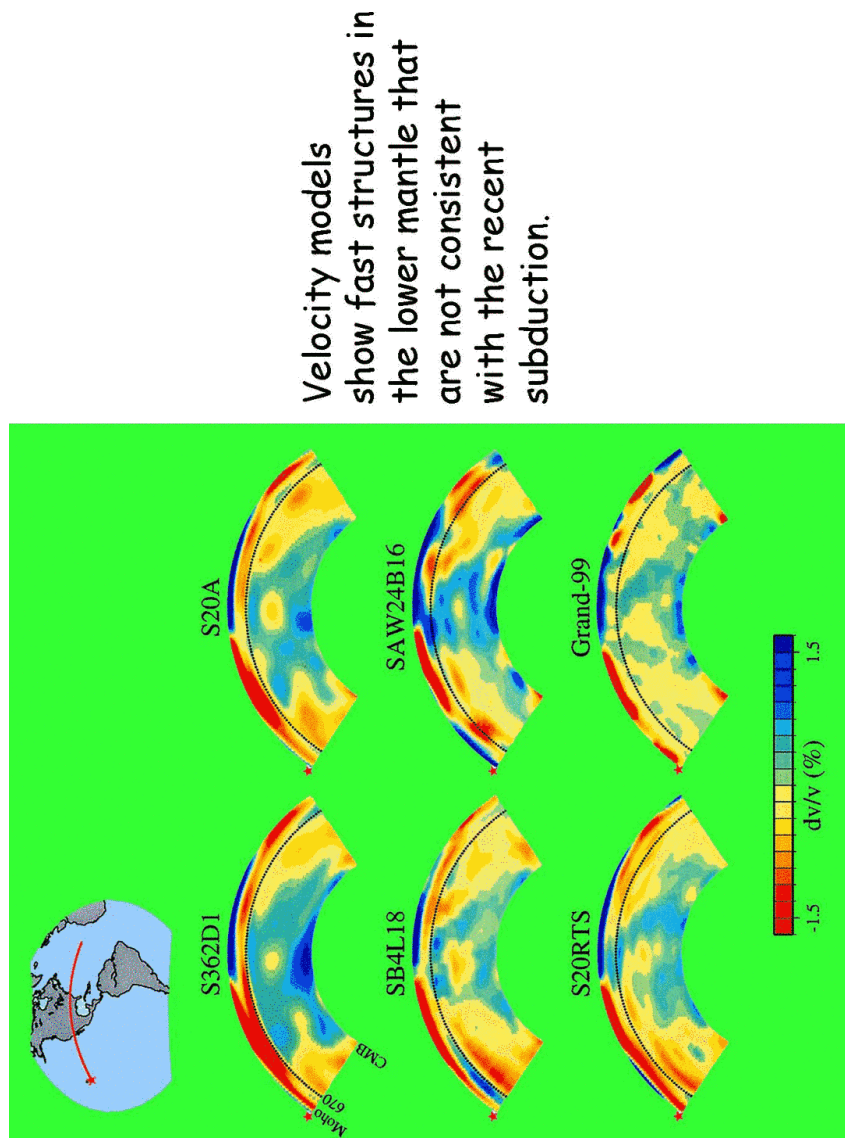
Chen & Brudzinski (2001)

Seismicity in the Tonga-Fiji-Vanuatu region shows great complexity, including earthquakes outside the Wadati-Benioff zones.

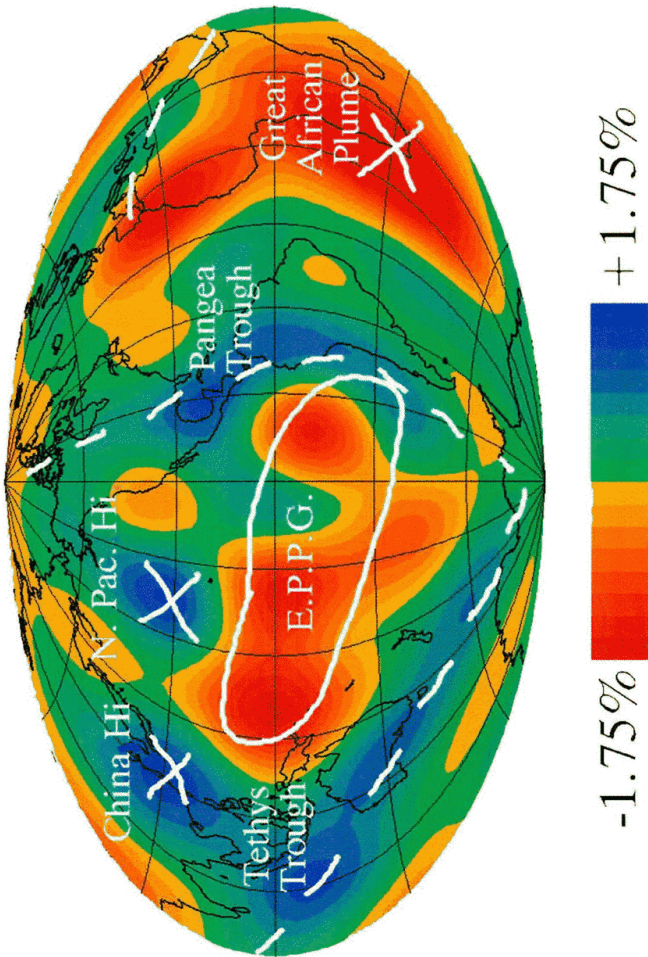


Fiji avalanche simulation

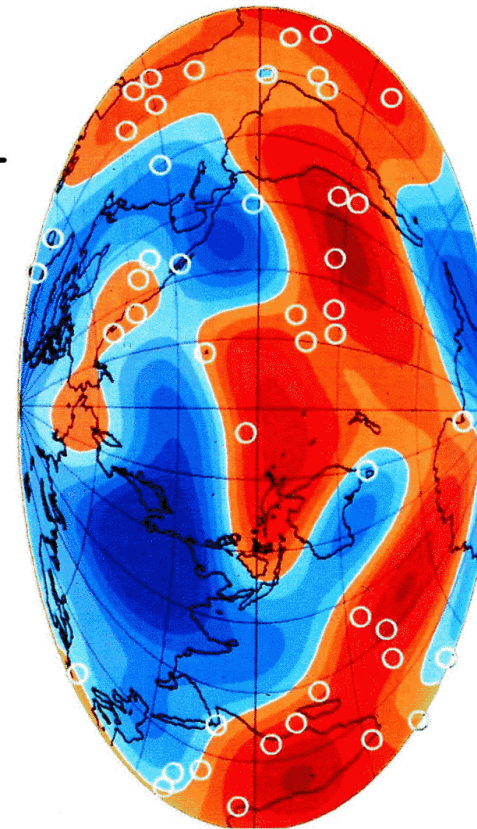
Pysklywec et al. (2003) have proposed that the tectonics of the Fiji Basin for the last 10 My can be explained by the occurrence of an avalanche caused by the breakthrough of a stagnant slab



Megastructures of the Earth's Interior

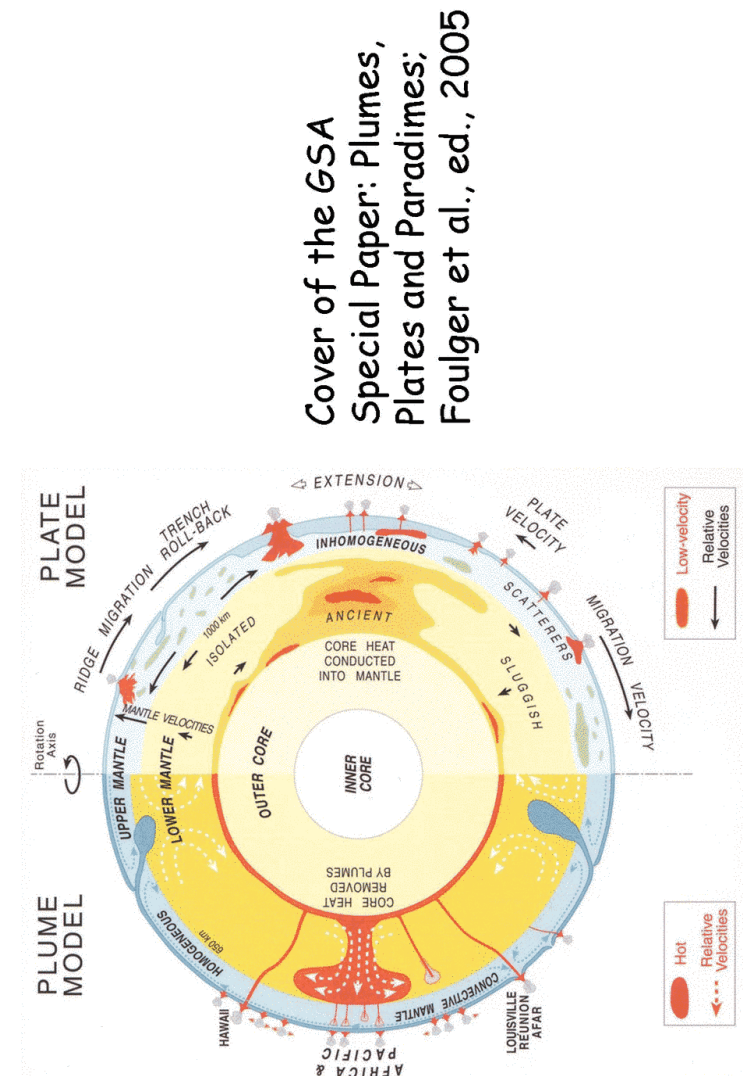


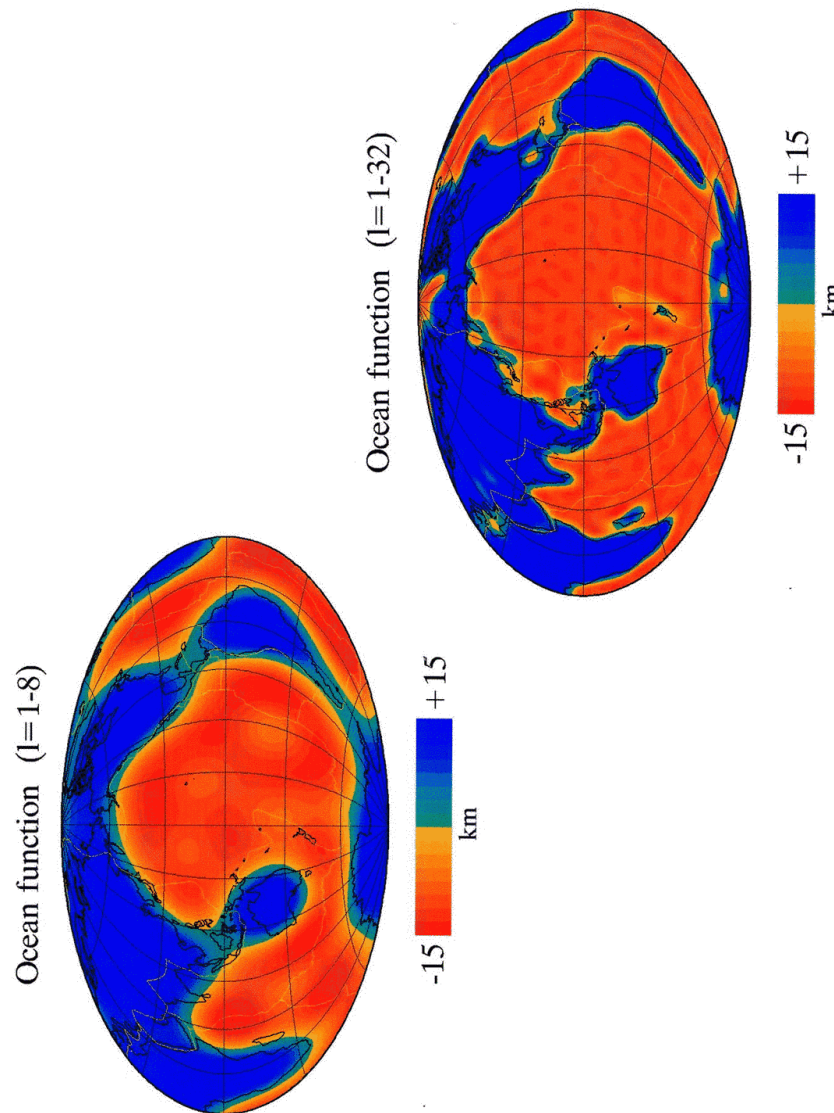
Lowermost mantle velocity anomalies
and distribution of hotspots



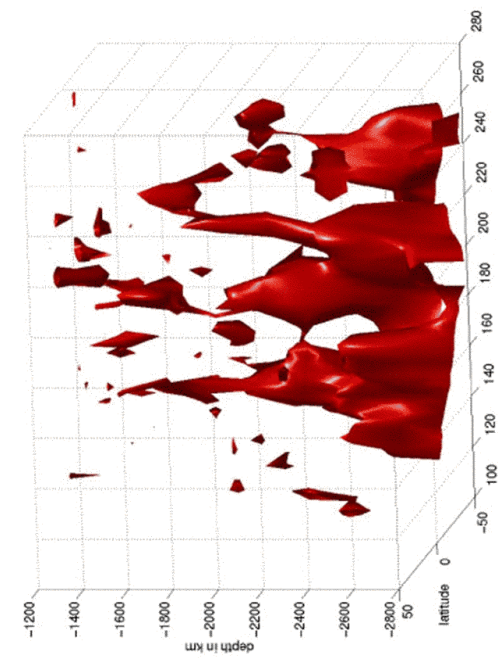
Surface locations of hotspots correspond closely to
the distribution of slow velocity anomalies near
core-mantle boundary (2750 km depth)

Six blind men and the Elephant

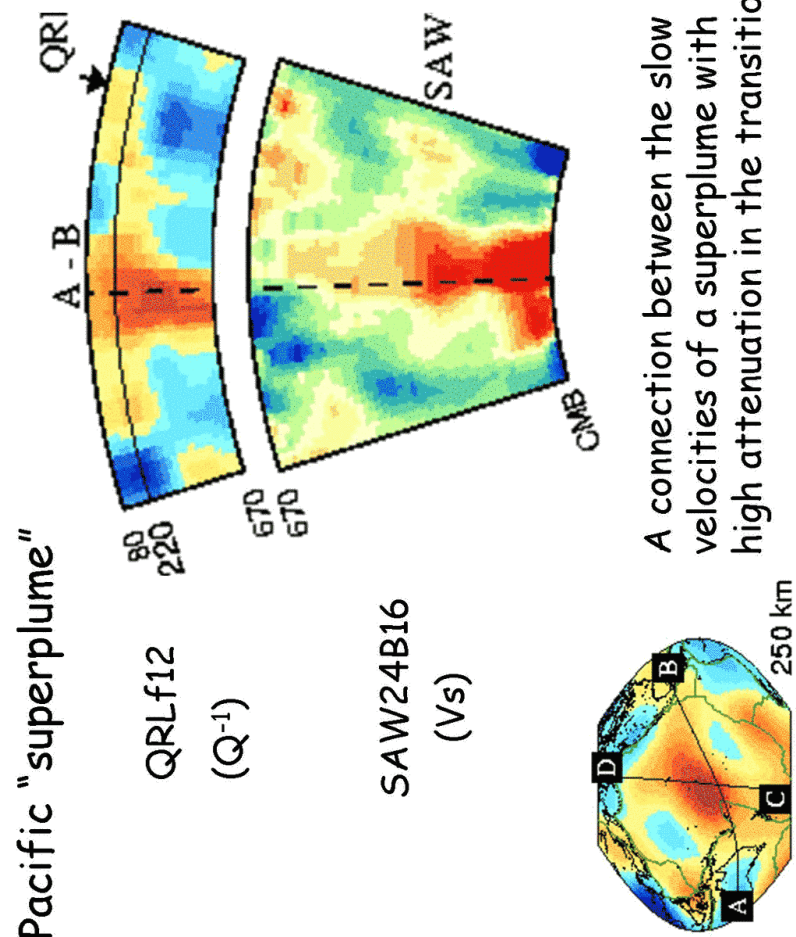




Equatorial Pacific Plume Group



The Pacific super-plume shows structure in this 3-D expansion of the -1% iso-surface of a recent Scripps model of shear velocity anomalies.



A connection between the slow
velocities of a superplume with
high attenuation in the transition zone

Romanowicz and Gung, 2002

The Blind Men and the Elephant
by John Godfrey Saxe

*It was six men of Indostan
to learning much inclined,
Who went to see the Elephant
(though all of them were blind),
That each by observation
might satisfy his mind.*

*And so these men of Indostan
disputed loud and long,
Each in his own opinion
exceeding stiff and strong,
Though each was partly in the right,
and all were in the wrong!*

Moral:

*So oft in theologic wars,
the disputants, I ween,
Rail on in utter ignorance
of what each other mean,
And prate about an Elephant
not one of them has seen!*

Regional Avg. of TZ Thickness

